Biochimica et Biophysica Acta 1778 (2008) 2395–2404

Contents lists available at ScienceDirect

Biochimica et Biophysica Acta

journal homepage: www.elsevier.com/locate/bbamem

A novel agonist effect on the nicotinic acetylcholine receptor exerted by the anticonvulsive drug Lamotrigine

Ana Sofía Vallés, Ingrid Garbus, Silvia S. Antollini, Francisco J. Barrantes *

UNESCO Chair of Biophysics and Molecular Neurobiology and Instituto de Investigaciones Bioquímicas de Bahía Blanca, C.C. 857, B8000FWB Bahía Blanca, Argentina

ARTICLE INFO

Article history:
Received 18 April 2008
Received in revised form 13 June 2008
Accepted 17 June 2008
Available online 24 June 2008

Keywords:
Lamotrigine
AChR
APL
αBTX
Agonist

ABSTRACT

The anticonvulsive drug Lamotrigine (LTG) is found to activate adult muscle nicotinic acetylcholine receptors (AChR). Single-channel patch-clamp recordings showed that LTG (0.05–400 μM) applied alone is able to open AChR channels. [^{125}I]α-bungarotoxin-binding studies further indicate that LTG does not bind to the canonical ACh-binding sites. Fluorescence experiments using the probe crystal violet demonstrate that LTG induces the transition from the resting state to the desensitized state of the AChR in the presence of excess α-bungarotoxin, that is, when the agonist site is blocked. Allosterically-potentiating ligands or the open-channel blocker QX-314 exhibited a behavior different from that of LTG. We conclude that LTG activates the AChR through a site that is different from those of full agonists/competitive antagonists and allosterically-potentiating ligands, respectively.

1. Introduction

Nicotinic acetylcholine receptors (AChRs) are pentameric oligomers present in neuronal and non-neuronal cells [1–3]. There has been growing interest in the study of receptor ligands owing to the involvement of AChRs in a variety of central nervous system disorders such as epilepsy, Alzheimer's disease and Parkinson's disease [4–7].

In recent years a number of unconventional ligands that modulate AChR activity have been discovered. Galantamine and physostigmine are representative compounds within this class, termed allosterically-potentiating ligands (APL) [8]. Both drugs are plant-derived inhibitors of acetylcholinesterase and have been used for symptomatic treatment of Alzheimer's disease [9]. These drugs can activate and potentiate AChR function [9–12]. Evidence suggests that APL-like molecules open the AChR channel by binding to a site different from that of canonical nicotinic agonists. Furthermore, photoaffinity labeling studies using [^{3}H]physostigmine demonstrated labeling of Lys^{125} in the *Torpedo* AChR α subunit, suggesting that this residue may participate in the APL–AChR interaction [13] even though this amino acid is not part of the nicotinic agonist binding site.

Lamotrigine (LTG) is an anticonvulsive drug used in the treatment of partial epilepsies. The major pharmacological effect of LTG reported to date is the blockage of voltage-dependent sodium channel conductance [14–17]. Recent studies from our laboratory showed that in the presence of ACh, LTG behaves as a typical muscle AChR open-channel blocker [18]. Here LTG is shown to be an activator of the adult-type muscle AChR channel, acting through a site that is different from that of nicotinic agonists, competitive antagonists and APL-type molecules.

2. Materials and methods

2.1. Chemicals

Lamotrigine (6-(2,3-dichlorophenyl) 1,2,4-triazine-3, 5-diamine) was purchased from GlaxoSmithKline (Co. Durham, UK). Carbamoylcholine chloride (Carb) and acetylcholine chloride (ACh) were purchased from Sigma and stored at −20 °C in a 10 mM aqueous stock solution. Crystal Violet (CrV) was purchased from Sigma-Aldrich (St. Louis, MO). Alpha-bungarotoxin (αBTX) was purchased from Sigma; [^{125}I] was purchased from New England Nuclear (Boston, MA) and [^{125}I]αBTX was prepared in our laboratory by radioiodination of cold αBTX using the chloramine-T method [19]. The specific activity of [^{125}I]αBTX was estimated to be 25 μCi/nmol.

2.2. Cell culture

CHO-K1/A5 is a cell line developed in our laboratory [20] that expresses adult muscle-type AChR. Cells were cultured in Ham's-F12 medium supplemented with 10% bovine fetal serum and 40 mg/ml of the selection antibiotic G418 (Sigma) in the medium.

2.3. Single-channel recordings

Single-channel currents were recorded in the cell-attached configuration [21] at a membrane potential of −80 mV and 20 °C

* Corresponding author. Tel.: +54 291 4861201; fax +54 291 4861200.
E-mail addresses: rtfjb1@criba.edu.ar, rtfjb1@yahoo.com (F.J. Barrantes).

0005-2736/$ – see front matter © 2008 Elsevier B.V. All rights reserved.
doi:10.1016/j.bbamem.2008.06.012

using an Axopatch 200B patch-clamp amplifier (Axon Instruments, Inc., CA), digitized at 94 kHz with an ITC-16 interface (Instrutech Corporation, Long Island, NY) and transferred to a computer using the program Acquire (Bruxton Corporation, Seattle, WA). The bath and pipette solutions contained 142 mM KCl, 5.4 mM NaCl, 1.8 mM $CaCl_2$, 1.7 mM $MgCl_2$ and 10 mM HEPES (pH 7.4). Patch pipettes were pulled from Kimax-51 capillary tubes (Kimble Products, Vineland, NJ), coated with Coat D (M-Line accessories, Measurements Group, Raleigh, NC), and fire-polished. Pipette resistances ranged from 5 to 7 MΩ. LTG was prepared from a 10 mM stock solution in ethanol, stored at −20 °C. ACh working solutions (30 μM) were dissolved in the bath solution from a 10 mM stock solution which was normally kept stored at −20 °C. Following ethanol evaporation under a stream of N_2, LTG was dissolved in the bath solution (0.05–400 μM) and then applied to the channel from the pipette tip. Detection of single-channel events using the program TAC followed the half-amplitude threshold criterion (Bruxton Corporation, Seattle WA) at a bandwidth of 5 kHz. The sampling time was 20 μs and the minimum detectable interval was 0.066 ms [22]. Open, burst and closed-time histograms were plotted using a logarithmic abscissa and a square root ordinate and fitted to the sum of exponential functions by the maximum likelihood criterion using the program TACFit (Bruxton Corporation, Seattle, WA). Burst resolution was obtained from the intersection between the main closed-time component and the succeeding one.

2.4. Whole-cell recordings

The extracellular solution contained 140 mM NaCl, 5 mM KCl, 1.8 mM $CaCl_2$, 1.7 mM $MgCl_2$ and 25 mM HEPES, pH 7.4, and the intracellular solution contained 145 mM KCl, 5 mM NaCl, 1 mM EGTA and 25 mM HEPES, pH 7.4. Pipette resistances ranged from 3 to 4 MΩ. Upon high-resistance sealing, cells were lifted from the bottom of the dish and ACh, LTG or extracellular solution was delivered using a Warner SF 77 Fast Step perfusion system (Warner instruments, Hamden, CT) under computer control. Using this setup, the solution around the cell could be completely exchanged within 10–15 ms. Whole-cell currents were recorded at different holding potentials at 20 °C using an Axopatch 200B and transferred to a computer using the program PULSE (HEKA GmbH, Lambrecht, Germany). The cells were exposed to the agonist flow for 2 s and washed with medium to enable multiple recordings while avoiding significant desensitization. Currents were measured every 2–3 min. LTG and ACh were applied to different cell dishes.

2.5. Fluorescence microscopy

CHO-K1/A5 cells were grown on 25 mm diameter glass coverslips in Ham's-F 12 medium for 2–3 days at 37 °C. Cells were washed twice with M1 buffer (150 mM NaCl, 1 mM $CaCl_2$, 1 mM $MgCl_2$, and 5 mM KCl in 20 mM HEPES buffer, pH 7.4) and stained for 1 h on ice with Alexa $Fluor^{488}$-αBTX at a final concentration of 1 μM. Cells were then rinsed three times with M1, mounted, and imaged using a wide-field Nikon Eclipse E-600 microscope using a 60× (1.4 N.A.) or 40× (1.0 N.A.) objective and digitized with a model ST-7 SBIG digital charge-coupled device camera (765×510 pixel, 9.0×9.0 mm pixel size; Santa Barbara, CA), thermostatically cooled at −10 °C. The ST-7 CCD camera was driven by the CCDOPS software package (SBIG Astronomical Instruments, version 5.02). Appropriate dichroic and emission filters were employed to avoid crossover of fluorescence emission. Background images were acquired from areas without cells from the same specimen and 16-bit TIFF images were exported for further off-line analysis. Fluorescence images were analyzed with the software Scion Image version 4.0.2 (Scion Corporation, Frederic, MD). The average fluorescence intensity over distinct areas of the cell surface was calculated for cells chosen at random for each experimental condition.

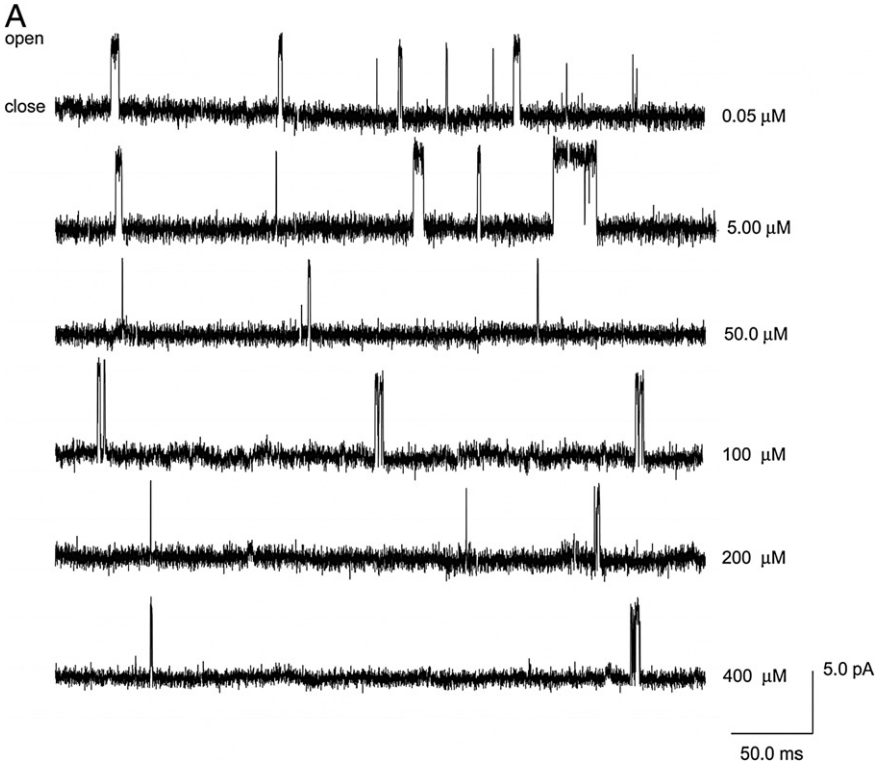

Fig. 1. LTG exerts agonist (at low concentration) and inhibitory (at high concentration) effects on muscle AChR. (A) Raw single-channel traces and (B) open (left), bursts (centre) and closed (right) time histograms of single-channel recordings obtained in the cell-attached configuration from CHO-K1/A5 cells expressing adult AChR. Membrane potential: −80 mV. Filter: 5 kHz.

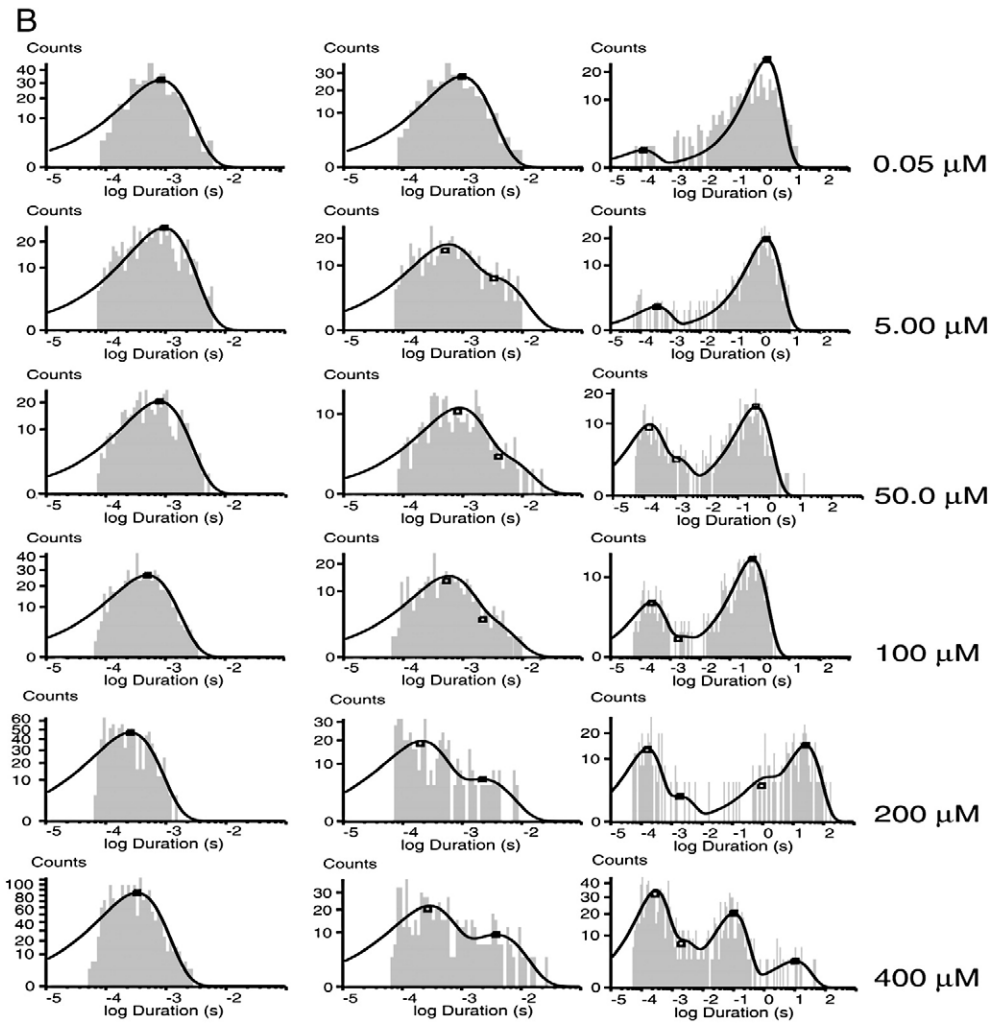

Fig. 1 (*continued*).

2.6. Ligand binding assays

LTG binding to the AChR was determined using a [^{125}I]αBTX binding assay. CHO-K1/A5 cells were re-suspended in high potassium Ringer's solution. Cells were pre-incubated for 30 min in the absence or presence of LTG (10^{-4}–10^{3} μM) or αBTX (10^{-4}–10 μM) or Carb (10^{-2}–10^{6} μM) and [^{125}I]αBTX was added to a final concentration of 20 nM for an additional 60 min. Binding was stopped by centrifugation for 5 min at 2000×*g*. Each experiment was carried out twice in triplicate and results were analyzed by normalizing to the binding in the absence of any competitive ligand. Radioactivity was measured in a gamma counter with an efficiency of 80%.

2.7. Fluorescence assay of AChR conformational states

Membrane fragments rich in AChR were prepared from the electric tissue of *T. californica* as previously described [23]. Specific activities in the order of 2.0–2.8 nmol αBTX sites/mg protein were obtained. The orientation of AChR in the membrane vesicles was determined by comparing the total toxin-binding sites in the presence of Triton X-100 and the right-side-out toxin-binding sites in the absence of detergent [24–25]. For the fluorescence measurements, AChR-rich membranes were suspended in buffer A (150 mM NaCl, 0.25 mM $MgCl_2$, and 20 mM HEPES buffer, pH 7.4) at a final concentration of 100 μg protein/mL (0.4 μM in terms of toxin-binding sites).

Fluorescence measurements were performed in an SLM model 4800 fluorimeter (SLM Instruments, Urbana, IL) using a vertically polarized light beam from a Hannovia 200-W mercury/xenon arc obtained with a Glan-Thompson polarizer (4-nm excitation and emission slits) and 2 mL quartz cuvettes. The temperature was set at 25 °C with a thermostated circulating water bath (Haake, Darmstadt, Germany). Increasing quantities of CrV were added to the samples from an aqueous solution; after each addition the emission spectra were collected (excitation wavelength: 600 nm; scanning from 605 to 700 nm). From the emission spectrum collected in the presence of CrV, a spectrum obtained from the same cuvette before CrV addition (background) was subtracted and the maximum intensity (at 624 nm) was measured. For experiments carried out on desensitized AChR, 1 mM Carb was added 15 min before titration with CrV.

2.8. Data analysis

Data are expressed as mean±S.D. from independent experiments. Statistical analysis was performed using Student's *t* test.

3. Results

3.1. LTG activates the muscle-type AChR

Single-channel studies were performed on CHO-K1/A5 cells to evaluate the effect of the anticonvulsive drug LTG on AChR channel

Table 1
Single-channel kinetic parameters of Lamotrigine at membrane potential − 80 mV

LTG [μM]	τ_{open} (ms)	Amplitude (pA)	τ_{close1} (ms)	τ_{close1} relative weight	$\tau_{blocked}$ (ms)	$\tau_{blocked}$ relative weight
0.05 (n=3)	0.90±0.08	6.36±0.07	0.38±0.28	0.04±0.02	–	–
0.10 (n=5)	0.92±0.13	6.75±0.38	0.11±0.05	0.03±0.01	–	–
0.25 (n=3)	0.96±0.07	5.82±0.01	0.27±0.01	0.06±0.00	–	–
1.00 (n=6)	0.92±0.08	6.00±0.35	0.33±0.11	0.08±0.03	–	–
2.50 (n=4)	0.87±0.08	6.18±0.28	0.27±0.04	0.04±0.01	–	–
5.00 (n=3)	0.77±0.14	5.86±0.34	0.20±0.04	0.08±0.02	–	–
20.0 (n=4)	0.71±0.11*	6.12±0.13	0.20±0.06	0.13±0.03**	–	–
50.0 (n=5)	0.63±0.09**	6.44±0.09	0.20±0.05	0.44±0.17**	1.60±0.66	0.08±0.02
100 (n=6)	0.40±0.06**	6.09±0.47	0.19±0.05	0.28±0.12**	1.67±0.81	0.08±0.05
200 (n=3)	0.29±0.06**	4.85±0.38	0.19±0.08	0.35±0.18*	1.58±0.64	0.13±0.03
400 (n=3)	0.26±0.05**	4.98±0.44	0.22±0.09	0.37±0.17*	1.24±0.58	0.08±0.06

* Statistically significant differences with respect to 0.05 μM LTG (p<0.05).
** Statistically significant differences with respect to 0.05 μM LTG (p<0.01).

kinetics. Using the cell-attached configuration, muscle-type AChRs were exposed to LTG in the concentration range 0.05 to 400 μM. Fig. 1A shows raw traces of currents elicited by LTG. LTG was found to activate the AChR at all concentrations tested, opening the AChR channel at sparse intervals (see Supplementary data). As shown in Table 1, at the lowest concentration range assayed (0.05–20 μM) the kinetic parameters of the LTG-activated channels proved to be similar to those observed in previous studies at low concentrations of the natural agonist ACh [18–26]. The distribution of single-channel openings fitted well to a single exponential function (Fig. 1B and Supplementary data). Two components contributed to τ_{burst} in most recordings at LTG concentrations above 2.5 μM. The longest component (~2 ms) probably reflects the occurrence of opening events in bursts in the presence of LTG, whereas the shortest in duration but of higher relative weight (relative amplitude <0.67) corresponds to individual openings (Fig. 1B and Supplementary data). Two main closed-time components were observed in the recordings (Fig. 1B and Supplementary data). The briefer, $\tau_{closed1}$, component is always present in AChR closed-time duration histograms and most likely corresponds to the reopening of the closed channel before it finally reaches either a desensitized or an unliganded state. The longest, $\tau_{closed2}$, is related to the number of channels in the patch [27].

We further analyzed the AChR channel behavior at higher LTG concentrations (50–400 μM). At these concentrations, in addition to causing the channel to open, LTG also caused a concomitant reduction in τ_{open} (Fig. 1, Table 1 and Supplementary data) that is likely attributable to channel block (see below). The presence of two components contributing to τ_{burst} was evident at these concentrations. The duration of the longest τ_{burst} was similar to that observed for low LTG concentrations. Interestingly, as the LTG concentration increased, a reduction in the duration of the shortest τ_{burst} component was observed (Fig. 1B). Increasing the drug concentration caused a concomitant increase in the number of openings per burst from 1.61 ± 0.15 (n=3) at 0.05 μM to 6.43±1.44 (n=3) at 400 μM LTG. Even though this change was statistically significant (Fig. 2), the extent of the effect caused by LTG was not as strong as that exerted by the natural agonist ACh (Fig. 2 and see Fig. 4B).

Analysis of the closed-time distributions obtained at high LTG concentrations provided additional diagnostic criteria. The relative weight of the briefer closed-time component was significantly higher than that obtained at lower LTG concentrations (Figs. 1 and 3, Table 1 and Supplementary data). This increase could be related to the grouping of AChR apertures induced by LTG, as visualized in the raw traces. A new minor component of ~1.50 ms was also observed (see Table 1). We interpret this new component as the result of the channel blocking events, and hence refer to it hereafter as $\tau_{blocked}$. The fact that the duration of the blocked state did not increase with LTG concentration suggests that the blocking mechanism involves single-liganded LTG, as observed with galantamine blockage of the AChR [11].

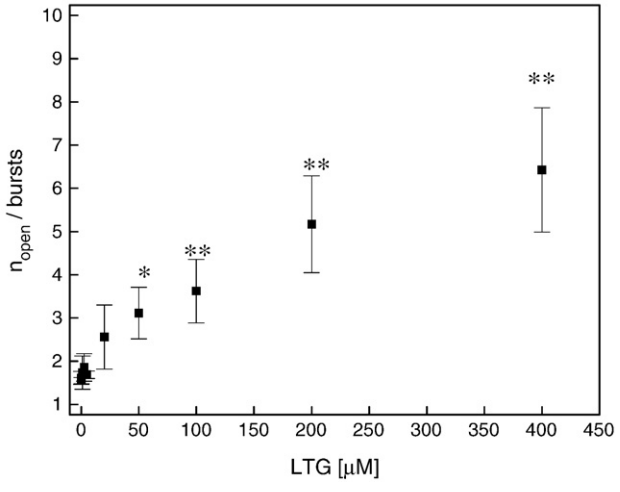

Fig. 2. Mean number of openings per bursts as a function of LTG concentration. Each point corresponds to the average±SD of at least three independent experiments. Statistically significant differences with respect to control values were indicated as follows: *p<0.01; **p< 0.007.

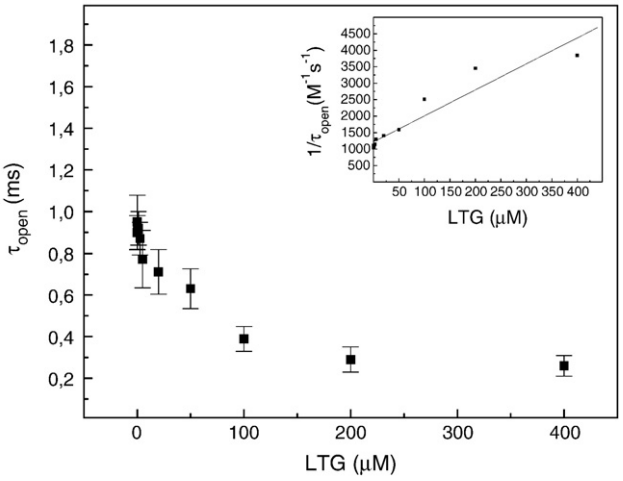

Fig. 3. Dependence of mean open time (τ_{open}) on LTG concentration. Values were extracted from the dwell-time histograms of single-channel data in the presence of LTG. Inset: reciprocal of τ_{open} vs. LTG concentration.

The channel amplitude was not significantly modified by LTG in the 0.05–400 μM concentration range (Table 1). At 200 and 400 μM, an additional closed-time component was apparent (Fig. 1B and Supplementary data). This component can be attributed to the desensitization, as commonly observed with other agonists at high concentrations [28].

3.2. LTG activates and blocks the muscle-type AChR

The blocking effect of LTG on AChR channels activated by the natural agonist AChR was accounted for in terms of a linear blocking mechanism [29–32] in a recent paper from our laboratory [18]. Here, the kinetics of channel blockage when AChR channels are activated with LTG (Fig. 3) are analyzed in terms of the classical sequential blocking scheme:

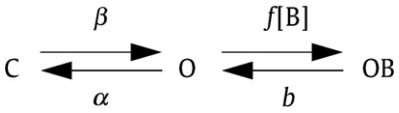

where C, O and OB represent the closed, open and open-blocked states of the AChR, respectively; α and β are the apparent closing and opening rate constants, respectively; f[B] and b are the apparent forward and backward rate constant for the blocking effect. The constants f[B], α and b were calculated to be 7.89×10^6 M^{-1} s^{-1}, 1219 s^{-1} and 611 s^{-1}, respectively. The resulting apparent dissociation constant for the blocking process, K_d, was 77.4 μM. No significant differences were apparent between these values and those found in the simultaneous presence of ACh and LTG [18].

3.3. LTG can activate whole-cell currents in muscle-type AChR

We asked next whether LTG could induce whole-cell currents in CHO-K1/A5 cells. We first obtained inwardly rectifying agonist-elicited currents after applying a 2 s pulse of 50 μM ACh at different membrane potentials (−80, −70 and −50 mV) to CHO-K1/A5 cells (Fig. 4A). Fig. 4A shows the induction of macroscopic whole-cell inward current responses after an application of a 2 s pulse of 100 μM LTG to another group of CHO-K1/A5 cells.

3.4. Effects of LTG on ACh-activated AChR channels

Given the dual action of LTG–AChR channel activator and inhibitor [18], we next focused on the characterization of ACh openings in the presence of LTG. For this purpose AChR channels were activated by ACh at a concentration that causes the channel to open in bursts. Wild-type AChRs open in well-defined activation episodes and subsequently desensitize at ACh concentrations above ~10 μM [33–34]. An activation episode starts with the transition of a single receptor from the desensitized to the activatable state and finishes upon returning to the desensitized state [33–34]. Using a pipette ACh concentration of 30 μM (Fig. 5A) AChR channels behaved as previously reported [26]. Channel opening distribution consisted of single openings that lasted ~1 ms. Three closed-time components were observed. The main component (relative weight 0.91±0.08) was fast, with an average duration of 0.60±0.11 ms. Two τ_{burst} components of equal contribution were observed, τ_{burst1} and τ_{burst2}, lasting 0.38±0.13 ms and 63±25 ms, respectively (Fig. 5B). The latter corresponds to the duration of a cluster.

We then co-applied 1 μM LTG with 30 μM ACh and channel kinetics were compared with those of 30 μM ACh alone. This LTG concentration was chosen because it activates the channel (Fig. 1B) but does not inhibit it in the presence of low ACh concentrations, as previously reported [18]. Under these conditions, τ_{open} was undistinguishable from that observed with ACh alone. However, although three closed-time components were also observed, their relative contribution varied notably (Fig. 5B). The most relevant finding became apparent with the τ_{burst} analysis. Firstly, although the duration of τ_{burst1} and τ_{burst2} remained unaltered, their relative contribution changed considerably. Thus the relative weight of τ_{burst1} increased with a concomitant decrease in τ_{burst2}. Secondly, a new component with a 1.97±0.58 ms duration, τ_{burst3}, was observed. This latter component can be attributed to the LTG-mediated induction of openings in groups.

As shown in Fig. 5C, the τ_{burst} histogram obtained using co-application of 30 μM ACh plus 1 μM LTG could be qualitatively fitted to the sum of the histograms obtained for the independent application of each drug, albeit changing the distribution but not the duration of τ_{burst}. The most plausible interpretation of this finding is that the equilibrium that allows the channel to open, close, reopen and finally close by desensitization, changes in the presence of LTG, shifting towards the shortest τ_{burst} component. Conversely, ACh did not affect the action of LTG, as reflected by the fact that the τ_{burst} component elicited by LTG alone could be distinguished from the τ_{burst} histogram obtained under co-application conditions. Clusters of openings were not observed when AChR channels were activated by LTG alone at any of the concentrations tested (Fig. 1A) as evidenced by the lack of any effect on the longest ACh-activated τ_{burst} component. This finding suggests that co-application of the full agonist together with LTG results in channel activation but does not promote cluster formation. To further test this hypothesis, another series of experiments was performed increasing the LTG concentration to 50 μM and again co-applying the drug with 30 μM ACh (Fig. 5B). This resulted in a slight

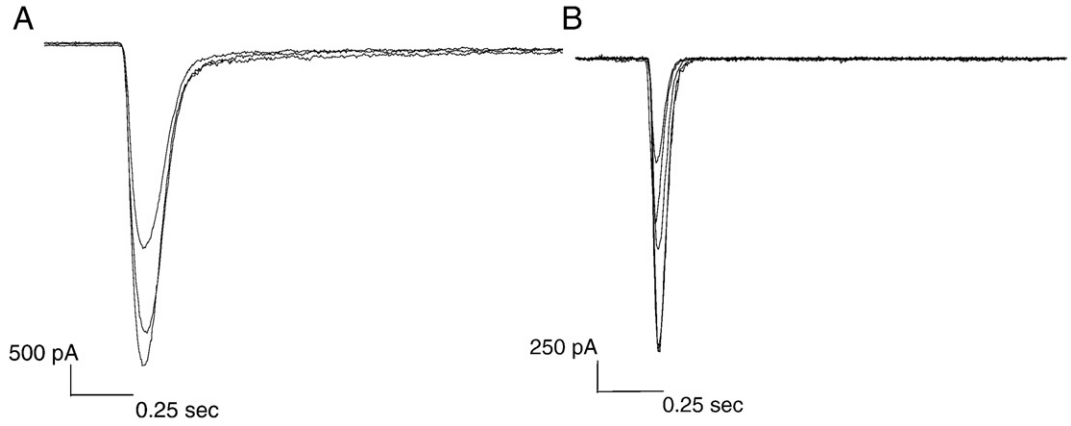

Fig. 4. LTG-generated currents. Whole-cell currents were recorded after application of a 2 s pulse of (A) 50 μM ACh at different membrane potentials (−80, −70 and −50 mV) and (B) 100 μM LTG at −110, −90, −80 and −70 mV.

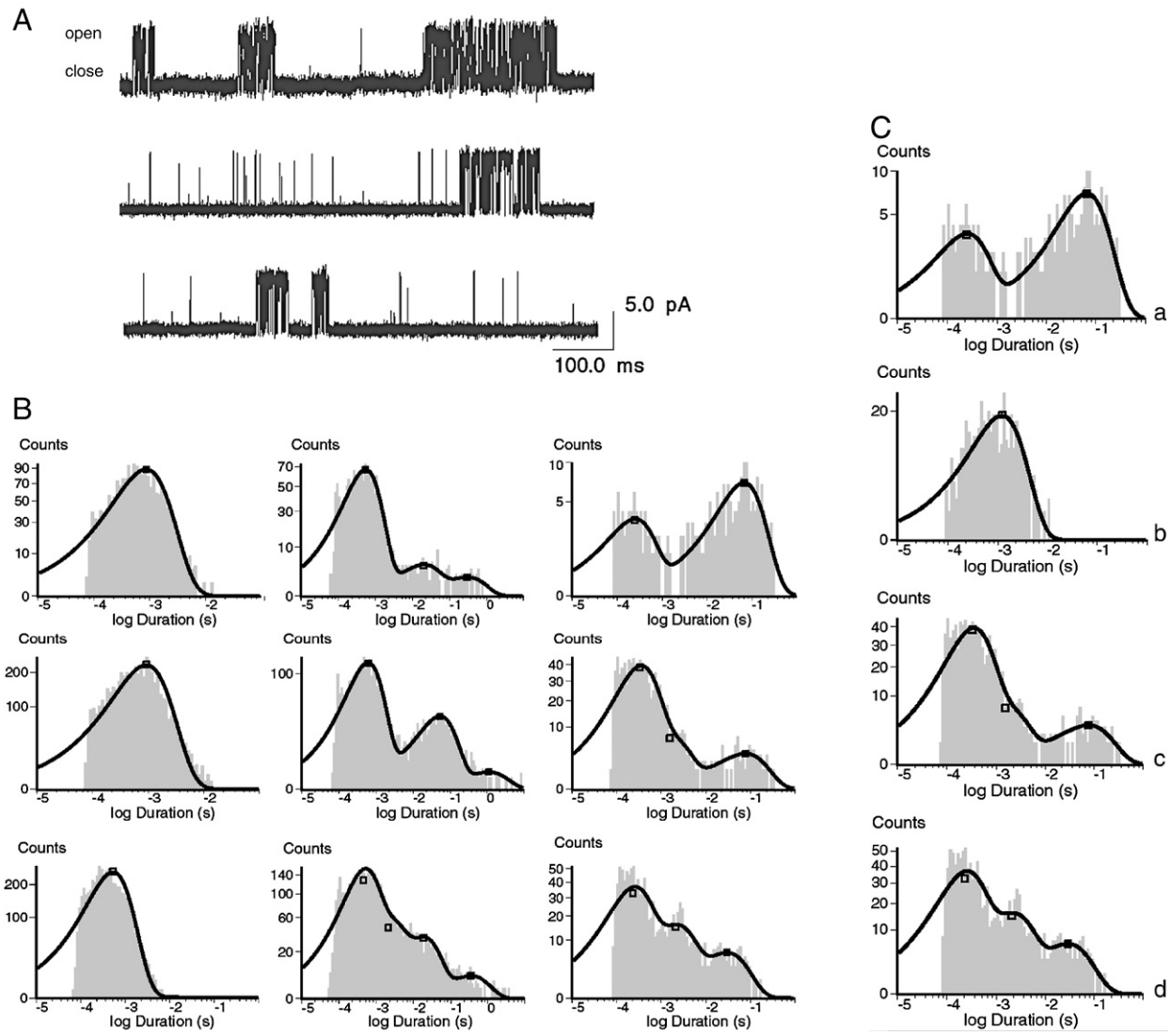

Fig. 5. LTG modifies AChR channel gating kinetics. Raw traces of single-channel recordings obtained in the cell-attached configuration from CHO-K1/A5 cells expressing adult AChR in the presence of (A) 30 μM ACh (upper row); 30 μM ACh + 1 μM LTG (middle row) and 30 μM ACh + 50 μM LTG (bottom row). (B) Open (first column), closed (second column) and burst (third column) time histograms resulting from the analysis of the recordings. (C) Comparison between burst time histograms resulting from the analysis of: (a) 30 μM ACh, (b)1 μM LTG, (c) 30 μM ACh + 1 μM LTG, and (d) 30 μM ACh + 50 μM LTG recordings. Membrane potential: −80 mV. Filter: 5 kHz.

reduction of τ_{open} as a consequence of channel block. A new component of τ_{closed} of ~2 ms became apparent. We infer that this new closed-time component most likely corresponds to $\tau_{blocked}$, as previously observed with LTG (50 to 400 μM). The main change observed was the relative increase in τ_{burst3}, thus reinforcing the above conclusion (Fig. 5C).

3.5. LTG induces the transition from the resting to the desensitized state of the Torpedo AChR

Having observed that LTG alone activates AChR channels, we studied next whether the presence of LTG induces the same type of conformational changes as classical agonists. Towards this end, fluorescence spectroscopy experiments were carried out using AChR-rich *Torpedo californica* membranes (in which more than 50% of the protein content corresponds to AChR protein) and the probe CrV. The latter is an aminotriarylmethane fluorescent dye that behaves as an AChR ion blocker and displays higher affinity for the AChR desensitized conformation (D) than for the AChR resting conformation (R) [35]. We took advantage of these differences in affinity to monitor changes in AChR conformational states in the presence of LTG (2.5–500 μM). CrV was directly titrated into a suspension of *Torpedo* AChR-rich membranes, and the apparent K_Ds were obtained by fitting the experimental values of CrV fluorescence to CrV concentration with a sigmoid equation (Fig. 6A). The control K_Ds of CrV in the R (without Carb) and D (with 1 mM Carb) states were 326.4 ± 31 and 43.8 ± 10 nM, respectively. When LTG was added to the membranes instead of Carb, the K_D of CrV decreased in a concentration-dependent manner with respect to the control value of the R state (Fig. 6B), and saturated at low LTG concentrations. The K_D of CrV calculated for membranes treated first with Carb and then with different concentrations of LTG was similar to that obtained with membranes treated with Carb alone. This series of experiments indicates that LTG effectively induces a state transition of the receptor, compatible with the behavior of an AChR agonist. Once this transition occurs, further addition of LTG causes no additional changes.

In order to dissect the dual behaviour of LTG, similar studies were performed with membranes previously incubated with the competitive antagonist αBTX at a concentration that effectively blocks the agonist binding site. The apparent K_D of CrV was similar to that observed for the R state in the presence of αBTX (Fig. 6B, inset). When the full agonist Carb was added after incubation of the membrane

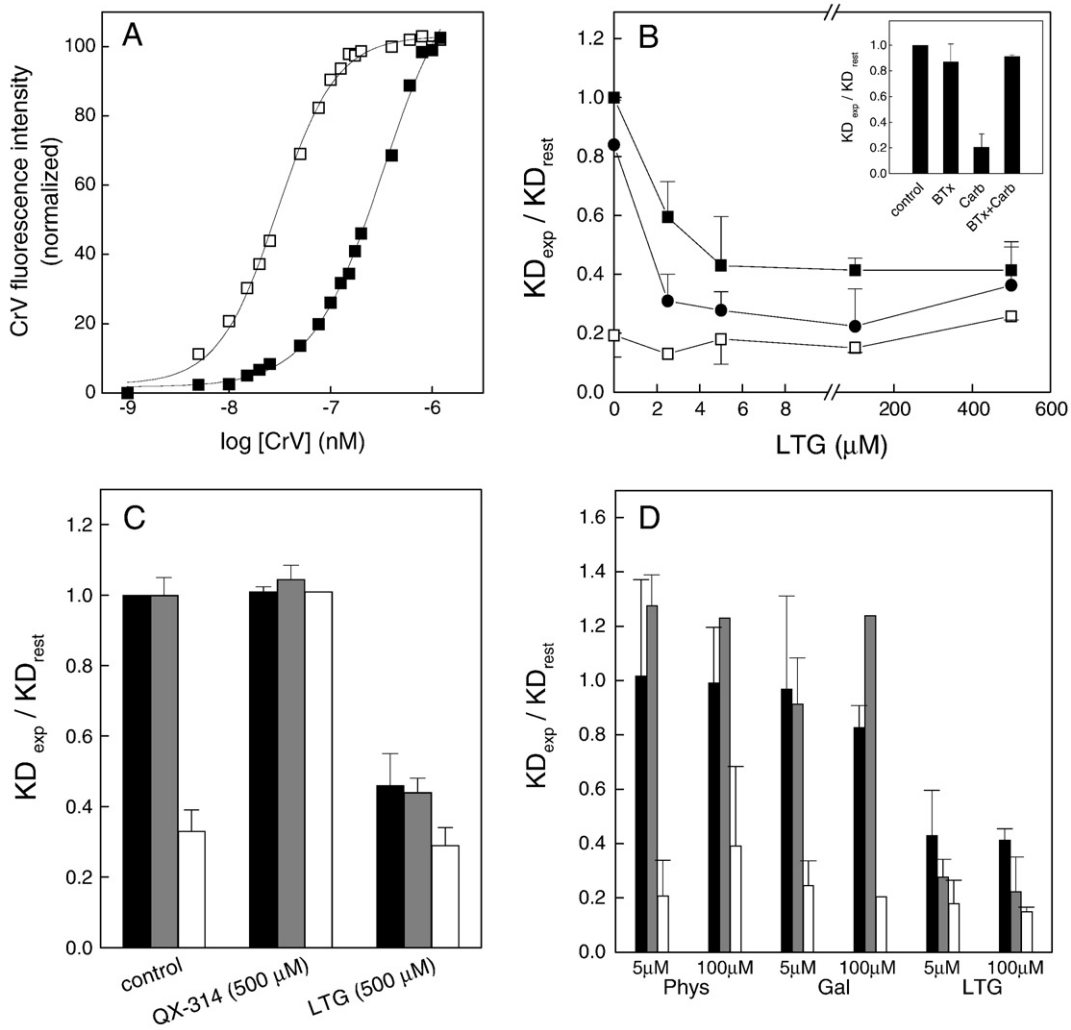

Fig. 6. (A) Specific fluorescence of CrV in the absence (■) or presence (□) of 1 mM Carb. CrV was directly titrated into a suspension of AChR-rich membranes from *Torpedo*. The apparent K_D's (see Results section) were obtained by fitting the experimental values of CrV fluorescence versus CrV concentration with a sigmoid equation (data from at least four separate experiments). (B) Variations in the K_D-ratio of the experimentally determined K_D values to the control K_D obtained in the resting state in the presence of increasing concentrations of LTG. The values were obtained with AChR-rich membrane alone (■), or in the presence of 1 mM Carb (□) or 1.5 μM αBTX (●). Inset: K_D-ratio calculated in the presence of 1 mM Carb, 1.5 μM αBTX or 1 mM Carb plus 1.5 μM αBTX. (C) Comparison between LTG and the ion channel blocker QX-314. The values were obtained with AChR-rich membranes alone (black columns), or in the presence of 1 mM Carb (white columns), or 1.5 μM αBTX (grey columns). (D) K_D-ratio calculated in the presence of physostigmine (5 and 100 μM), galantamine (5 and 100 μM) and LTG (5 and 100 μM) alone (black columns), or in the presence of 1 mM Carb (white columns) or 1.5 μM αBTX (grey columns). Each column/symbol corresponds to the average ± S.D. of at least four independent experiments.

with αBTX, the K_D of CrV did not change, indicating that the agonist binding sites were completely blocked (Fig. 6B, inset); however, when LTG was added subsequent to αBTX incubation the K_D of CrV decreased in a manner similar to that observed with LTG alone, indicating that LTG can activate the AChR even though the agonist binding sites are blocked (Fig. 6B). This result further suggests that the modulatory effect of LTG is exerted on different sites.

At high concentrations, LTG also behaves as an ion channel blocker, as is the case with CrV. One would thus expect that LTG competes with the fluorescence dye, displacing it from the ion pore, hence leading to an increase in K_D. However, this was not the case even at LTG concentrations as high as 500 μM, or using both αBTX and LTG (Fig. 6B). The canonical AChR channel blocker QX-314 was tested next for comparison (Fig. 6C). The K_D of CrV obtained in membranes treated with QX-314 alone, or after incubation with αBTX or Carb, was similar to that of the R state. The differences between the CrV-sensitive AChR states in the presence of 500 μM LTG or QX-314 confirm the observation that LTG has a dual effect on the AChR: at high concentrations, LTG not only acts as an ion channel blocker but also activates the AChR, the latter effect possibly being responsible for the AChR state transitions revealed here by CrV fluorescence spectroscopy experiments.

We studied next the effect of galantamine and physostigmine, two APL of the AChR, on the conformational equilibrium of the *Torpedo* AChR (Fig. 6D). Neither galantamine nor physostigmine alone induced changes in the K_D of CrV with respect to the control value for the R state. Furthermore, when these APL were added after incubation of the membranes with αBTX or Carb, the K_D of CrV did not change with respect to the controls, suggesting that LTG modulates the AChR through a mechanism different from that operating with APL.

3.6. LTG effects on the binding of αBTX to living CHO-K1/A5 cells

To corroborate that LTG binds to a different site from the ACh-binding site, two additional series of experiments were performed. First, the initial rate of [^{125}I]αBTX binding [36] was measured in CHO-K1/A5 cells after 30 min pre-incubation with LTG (10^{-4}–10^{3} μM). In the concentration range assayed, LTG did not affect [^{125}I]αBTX binding to the AChR (Fig. 7A). Similar experiments were performed after pre-incubation of cells with the full agonist Carb or the antagonist αBTX

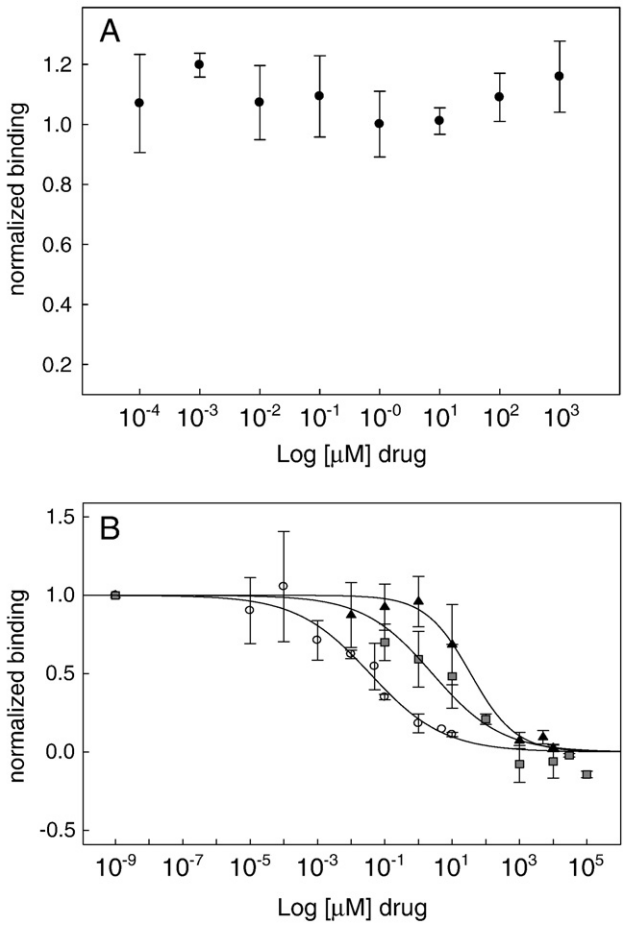

Fig. 7. (A) Initial rate of [^{125}I]αBTX binding to AChR in CHO-K1/A5 cells is not affected by LTG. (B) Reduction of the initial rate of [^{125}I]αBTX binding by the full agonist Carb (triangles), the competitive antagonist αBTX (circles), and Carb plus 100 μM LTG (squares).

(Fig. 7B). Both compounds inhibit [^{125}I]αBTX binding to the AChR. The IC_{50} for inhibition by Carb and αBTX were 35 μM and 36 nM, respectively (Fig. 7B). When LTG (100 μM) was applied together with different concentrations of Carb (Fig. 7B) the inhibition curve for Carb shifted to lower IC_{50} values (~2.6 μM) indicating that in the presence of LTG, Carb exhibits a higher affinity for the AChR.

To further confirm the lack of inhibition of [^{125}I]αBTX binding by LTG alone, Alexa Fluor^{488}αBTX staining of live CHO-K1/A5 cells was carried out (Fig. 8). 2 h incubation with 100 μM Carb significantly reduced cell-surface fluorescence (Fig. 8A, B), whereas the fluorescence intensity of cells incubated with concentrations as low as 50 μM LTG (Fig. 8C, D) or as high as 300 μM LTG under periods of up to 24 h, did not differ from that of control samples (Fig. 8E, F). These results indicate that LTG does not compete with the canonical competitive antagonist αBTX, in agreement with the fluorescence spectroscopy experiments (Fig. 6).

4. Discussion

A wide range of compounds has the ability to modulate the AChR. This modulation can be accomplished through different mechanisms, involving the agonist site, the pore itself, or amino acid residues in the transmembrane moiety of the AChR, the former and the latter mechanisms usually resulting in allosteric regulation [1,37]. ACh binds to the AChR at a well-defined pocket lined up with aromatic residues located at an interface between the α and non-α subunits.

In this work the effect of the anticonvulsive drug LTG on muscle AChRs was studied using a combination of single-channel and whole-cell patch-clamp recordings, fluorescence spectroscopy, fluorescence microscopy and radioligand binding strategies. The most notable finding of this work is that LTG, by itself, activates the muscle-type AChR at all concentrations tested, as evidenced by single-channel and whole-cell recordings (Figs. 1 and 4). Activation of the AChR by LTG exhibited several similarities with the action of the natural agonist, ACh. In agreement with the electrophysiological data, fluorescence spectroscopy experiments showed that upon binding to the AChR, LTG induces a transition from the resting (closed) state to the desensitized state. Altogether, these observations are compatible with an agonist effect of LTG.

At high LTG concentrations (50–400 μM) a blocking effect became evident, as previously observed in the case of ACh activation [18]. LTG caused (a) a decrease in channel mean open time (Fig. 1 and Supplementary data), (b) an increase in the mean burst duration (Fig. 1 and Supplementary data), (c) an increase in the number of openings per burst (Fig. 2) and (d) the appearance of a new closed channel component ("blocked time", Fig. 1). The duration of the latter remained constant at the concentrations tested (50–400 μM) whereas its relative weight showed a concentration-dependent behavior. In contrast to previous reports on the action of the open-channel blocking effect of tacrine on muscle-type AChR [38], a single LTG molecule appears to be involved since the duration of the closed state did not increase with LTG concentration. At the higher LTG concentrations tested (200 and 400 μM), desensitization became apparent with the appearance of a new closed-time component in the range of seconds (Fig. 1 and Supplementary data).

The simple channel-block model was used to describe the LTG blockage of LTG-activated channels. Inclusion of a desensitization pathway in this mechanistic description is not applicable because AChR mean open time diminishes as LTG concentration increases [18], and the high agonist concentrations required to obtain well-defined clusters of channel openings would result in complete channel blockage by LTG. The blocking action of LTG could be satisfactorily explained with this model in which the rapid dissociation of the drug shortens the channel open state and delays AChR closure, thus preventing transitions to the closed state leading to lengthier burst duration. No differences were found between the present analysis and the one satisfactorily describing the combined action of ACh and LTG [18] suggesting that the blocking potency of LTG is not influenced by the AChR-activating drug and that LTG activation and blocking are independent.

LTG was additionally found to modify τ_{close} and τ_{bursts} distribution of the AChR channel. Electrophysiological recordings obtained after application of ACh (30 μM) to the AChR showed that the channel opened preferentially in clusters and seldomly in the form of isolated openings, in contrast to what is observed at low ACh concentrations (1 μM). When LTG was co-applied with ACh a reduction in the relative weight of the fastest closed-time component was observed. This component is likely to correspond to the time spent by the channel in the closed state within a cluster. A concomitant increase in the amplitude of the faster of the two slow components, which corresponds to the duration of the channel in the closed state in between isolated openings, was also observed (Fig. 5). We interpret this phenomenon as resulting from LTG induced openings of the AChR. Furthermore, concentrations of LTG that cause blockage of the channel (50 μM) resulted in the appearance of $\tau_{blocked}$.

Piecing together the experimental evidence leads to the conclusion that LTG acts on sites different from those of nicotinic agonists, competitive antagonists or APL-type molecules, e.g. galantamine or physostigmine. LTG mimicked the response observed with a typical agonist (Carb) in fluorescence experiments even under conditions of αBTX blockage of the agonist binding sites, suggesting that the modulation of LTG occurs through a different site. LTG has two

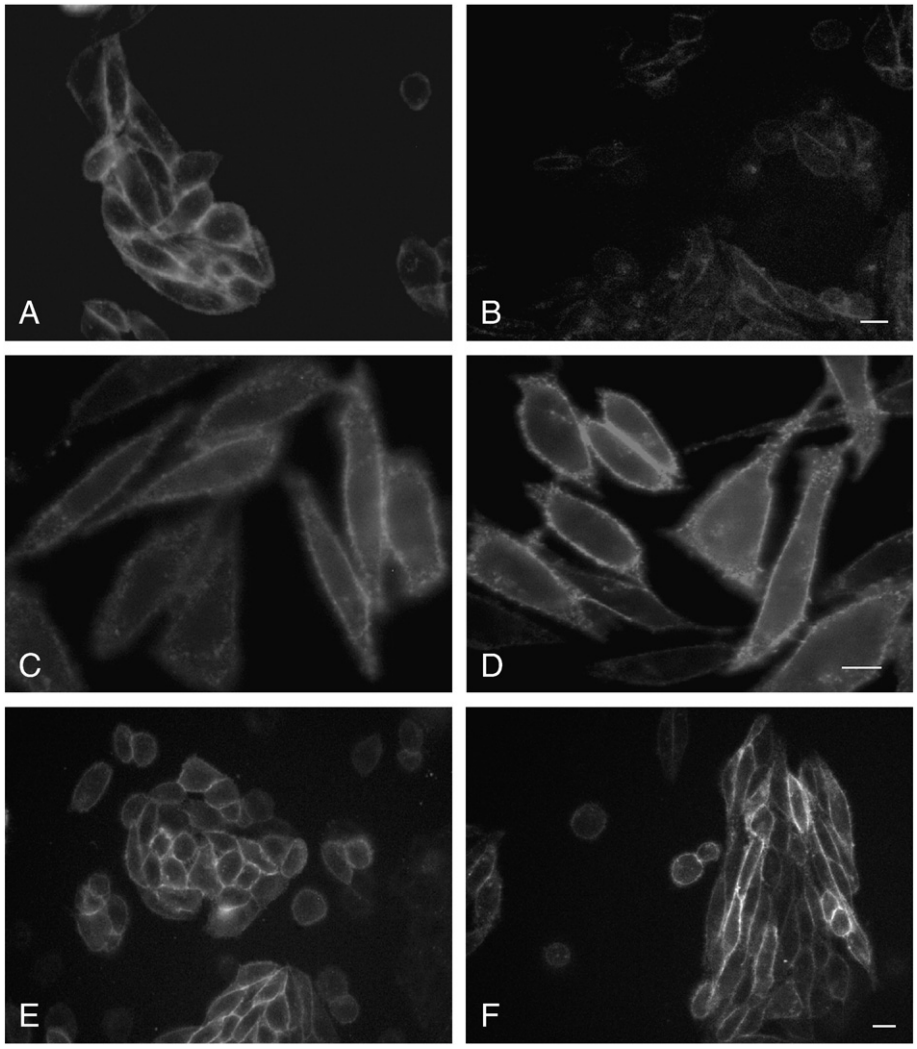

Fig. 8. Cell-surface αBTX fluorescence binding is not affected by LTG. CHO-K1/A5 cells were cultured in serum-free medium for 2 h in the absence (A and C) or presence of 100 μM Carb (B) or 50 μM LTG (D), or 24 h in the absence (E) or presence (F) of 300 μM LTG. Surface AChRs were stained with the fluorescent probe Alexa Fluor^{488}-αBTX. The bar indicates 10 μm.

ionizable groups, and ion pair formation between AChR and LTG could be responsible for the agonist effect; however, this possibility can be discarded because LTG at pH 7.4 is in its non-ionized form [39].

QX-314, a well known open-channel blocker of the AChR, did not modify the K_D of CrV in *Torpedo californica* AChR-rich membranes by itself or in the presence of αBTX or Carb, suggesting that the transitions made apparent by CrV fluorescence changes are the result of LTG acting as an activator rather than as a channel blocker. These results are fully compatible with the inability of LTG to inhibit the initial rate of [^{125}I]αBTX binding (Fig. 7). Similarly, fluorescence microscopy studies showed that Alexa^{488}αBTX cell-surface staining was not affected by LTG (Fig. 8). Collectively, the results support the hypothesis that LTG binds to a site different from the canonical agonist- and competitive antagonist-recognition site.

We further compared the effects of the most common APL-type molecules, galantamine and physostigmine, with those of LTG. Both drugs have previously been reported to activate the muscle AChR [11,12]. Activation apparently proceeds through sites distinct from those for nicotinic agonists and antagonists. No similarities were observed between the desensitizing properties of LTG and those of galantamine or physostigmine (Fig. 6D). A marked difference between LTG on the one hand and galantamine and physostigmine on the other is the fact that LTG elicited whole-cell currents by itself whereas the latter drugs do not [40–41]. Additionally, marked differences exist between the solubility properties of the two APL (water soluble) and LTG (soluble in organic solvents), further reinforcing the idea that LTG probably binds to a site different from that of the APL and has a different degree of hydrophobicity.

Finally, the results presented in Fig. 7 provide additional evidence that LTG alone can desensitize the AChR. Radioligand binding experiments demonstrated that when LTG was applied together with increasing concentrations of Carb, the IC_{50} for inhibition by Carb was reduced from ~35 μM to ~2.6 μM, indicating that in the presence of LTG, Carb exhibits higher affinity for the AChR [36,42].

In conclusion, the drug LTG makes apparent a new mode of AChR activation, which differs from that of the classical agonists and APL. Although AChRs are not the specific targets for the anticonvulsive action of LTG, experiments are now in progress to investigate whether some of the collateral effects of LTG in the central nervous system can be accounted for by the effect of this drug on neuronal AChRs.

Acknowledgements

Thanks are due to Dr. M. F. Pediconi for her help with ligand binding experiments. The research described in this article was supported in part by PICT 01-12790 and 5-20155 from Ministry of Science and Technology; PIP No. 6367 from the Argentinian Scientific Research Council (CONICET); Philip Morris USA Inc. and Philip Morris

International; and PGI No. 24/B135 from Universidad Nacional del Sur, Argentina, to F.J.B.

Appendix A. Supplementary data

Supplementary data associated with this article can be found, in the online version, at doi:10.1016/j.bbamem.2008.06.012.

References

[1] J.P. Changeux, A. Devillers-Thiery, P. Chemouilli, Acetylcholine receptor: an allosteric protein, Science 225 (1985) 1335–1345.
[2] R. Anand, W.G. Conroy, R. Schoepfer, P. Whiting, J. Lindstrom, Neuronal nicotinic acetylcholine receptors expressed in *Xenopus oocytes* have a pentameric quaternary structure, J. Biol. Chem. 266 (1991) 11192–11198.
[3] J.L. Galzi, J.P. Changeux, Neuronal nicotinic receptors: molecular organization and regulations, Neuropharmacology 34 (1995) 563–582.
[4] F.J. Barrantes, The acetylcholine receptor ligand-gated channel as a molecular target of disease and therapeutic agents, Neurochem. Res. 22 (1997) 391–400.
[5] F.J. Barrantes, E. Aztiria, M.B. Rauschemberger, A. Vasconsuelo, The neuronal nicotinic acetylcholine receptor in some hereditary epilepsies, Neurochem. Res. 25 (2000) 583–590.
[6] C. Gotti, F. Clementi, Neuronal nicotinic receptors: from structure to pathology, Prog. Neurobiol. 74 (2004) 363–396.
[7] A.A. Jensen, B. Frolund, T. Liljefors, P. Krogsgaard-Larsen, Neuronal nicotinic acetylcholine receptors: structural revelations, target identifications, and therapeutic inspirations, J. Med. Chem. 48 (2005) 4705–4745.
[8] E.F. Pereira, C. Hilmas, M.D. Santos, M. Alkondon, A. Maelicke, E.X. Albuquerque, Unconventional ligands and modulators of nicotinic receptors, J. Neurobiol. 53 (2002) 479–500.
[9] A. Maelicke, E.X. Albuquerque, Allosteric modulation of nicotinic acetylcholine receptors as a treatment strategy for Alzheimer's disease, Eur. J. Pharmacol. 393 (2000) 165–170.
[10] A. Maelicke, T. Coban, A. Storch, A. Schrattenholz, E.F. Pereira, E.X. Albuquerque, Allosteric modulation of *Torpedo* nicotinic acetylcholine receptor ion channel activity by noncompetitive agonists, J. Recept. Signal Transduct. Res. 17 (1997) 11–28.
[11] G. Akk, J.H. Steinbach, Galantamine activates muscle-type nicotinic acetylcholine receptors without binding to the acetylcholine-binding site, J. Neurosci. 25 (2005) 1992–2001.
[12] K.P. Shaw, Y. Aracava, A. Akaike, J.W. Daly, D.L. Rickett, E.X. Albuquerque, The reversible cholinesterase inhibitor physostigmine has channel-blocking and agonist effects on the acetylcholine receptor–ion channel complex, Mol. Pharmacol. 28 (1985) 527–538.
[13] A. Schrattenholz, J. Godovac-Zimmermann, H.J. Schäfer, A. Maelicke, Photoaffinity labeling of *Torpedo* acetylcholine receptor by physostigmine, Eur. J. Biochem. 216 (1993) 671–677.
[14] M.J. Leach, C.M. Marden, A.A. Miller, Pharmacological studies on lamotrigine, a novel potential antiepileptic drug: neurochemical studies on the mechanisms of action, Epilepsia 25 (1986) 90–497.
[15] H. Cheung, D. Kamp, E. Harris, An in vitro investigation of the action of lamotrigine on neuronal voltage-activated sodium channels, Epilepsy Res. 13 (1992) 107–112.
[16] D.G. Lang, C.M. Wang, B.R. Cooper, Lamotrigine, phenytoin and carbamazepine interactions on the sodium current present in N4TG1 mouse neuroblastoma cells, J. Pharmacol. Exp. The. 266 (1993) 829–835.
[17] C. Zona, M. Avoli, Lamotrigine reduces voltage-gated sodium currents in rat central neurons in culture, Epilepsia 38 (1997) 522–525.
[18] A.S. Vallés, I. Garbus, F.J. Barrantes, Lamotrigine is an open-channel blocker of the nicotinic acetylcholine receptor, NeuroReport 18 (2007) 45–50.
[19] W.M. Hunter, F.C. Greenwood, Preparation of iodine-131 labelled human growth hormone of high specific activity, Nature 194 (1962) 495–496.
[20] A.M. Roccamo, M.F. Pediconi, E. Aztiria, L. Zanello, A. Wolstenholme, F.J. Barrantes, Cells defective in sphingolipids biosynthesis express low amounts of muscle nicotinic acetylcholine receptor, Eur. J. Neurosci. 11 (1997) 1615–1623.
[21] O.P. Hamill, A. Marty, E. Neher, B. Sakmann, F.J. Sigworth, Improved patch-clamp techniques for high-resolution current recording from cells and cell-free membrane patches, Pflugers. Arch. 391 (1981) 85–100.
[22] D. Colquhoun, F.J. Sigworth, Fitting and statistical analysis of single-channel records, in: B. Sakmann, E. Neher (Eds.), Single-Channel Recording, Plenum Publishing Corp., New York, 1983, pp. 191–263.
[23] F.J. Barrantes, Interactions between the acetylcholine receptor and the non-receptor, peripheral nu-peptide (Mr 43,000), in: F. Hucho (Ed.), Neuroreceptors, W. de Gruyter, Berlin, 1982, pp. 315–328.
[24] P.R. Hartig, M.A. Raftery, Preparation of right-side-out, acetylcholine receptor enriched intact vesicles from *Torpedo californica* electroplaque membranes, Biochemistry 18 (1979) 1146–1150.
[25] C. Gutierrez-Merino, I.C. Bonini de Romanelli, L.I. Pietrasanta, F.J. Barrantes, Preferential distribution of the fluorescent phospholipid probes NBD-phosphatidylcholine and rhodamine-phosphatidylethanolamine in the exofacial leaflet of acetylcholine receptor-rich membranes from *Torpedo marmorata*, Biochemistry 34 (1995) 846–4855.
[26] I. Garbus, A.M. Roccamo, F.J. Barrantes, Identification of threonine 422 in transmembrane domain alpha M4 of the nicotinic acetylcholine receptor as a possible site of interaction with hydrocortisone, Neuropharmacology 43 (2002) 65–73.
[27] S.M. Sine, J.H. Steinbach, Acetylcholine receptor activation by a site-selective ligand: nature of brief open and closed states in BC3H-1 cells, J. Physiol. 370 (1986) 357–379.
[28] A.B. Cachelin, D. Colquhoun, Desensitization of the acetylcholine receptor of frog end-plates measured in a Vaseline-gap voltage clamp, J. Physiol. (1989) 159–188.
[29] C.M. Armstrong, Interaction of tetraethylammonium ion derivatives with the potassium channels of giant axons, J. Gen. Physiol. 58 (1971) 413–437.
[30] P.R. Adams, Drug blockade of open end-plate channels, J. Physiol. 260 (1976) 531–552.
[31] D. Colquhoun, B. Sakmann, Fast events in single-channel currents activated by acetylcholine and its analogues at the frog muscle end-plate, J. Physiol. 369 (1985) 501–557.
[32] S.J. Robertson, P.A. Jennington, A.M. Evans, R.J. Martin, The action of pyrantel as an agonist and an open channel blocker at acetylcholine receptors in isolated *Ascaris suum* muscle vesicles, Eur. J. Pharmacol. 271 (1994) 273–282.
[33] B. Sakmann, J. Patlak, E. Neher, Single acetylcholine-activated channels show burst-kinetics in the presence of desensitizing concentrations of agonist, Nature 286 (1980) 71–73.
[34] A. Auerbach, G. Akk, Desensitization of mouse nicotinic acetylcholine receptor channels. A two-gate mechanism, J. Gen. Physiol. 112 (1998) 181–197.
[35] M.M. Lurtz, S.E. Pedersen, Aminotriarylmethane dyes are high-affinity noncompetitive antagonists of the nicotinic acetylcholine receptor, Mol. Pharmacol. 55 (1999) 159–167.
[36] S. Sine, P. Taylor, Functional consequences of agonist-mediated state transitions in the cholinergic receptor. Studies in cultured muscle cells, J. Biol. Chem. 254 (1979) 3315–3325.
[37] J.P. Changeux, Nicotinic Acetylcholine Receptors: from Molecular biology to Cognition, In: Odile Jacob (Ed.), Odile Publishing Corp., New York, 1983.
[38] R.J. Prince, R.A. Pennington, S.M. Sine, Mechanism of tacrine block at adult human muscle nicotinic acetylcholine receptors, J. Gen. Physiol. 120 (2002) 369–393.
[39] R. Mashru, V. Sutariya, M. Sankalia, J. Sankalia, Transbuccal delivery of lamotrigine across porcine buccal mucosa: in vitro determination of routes of buccal transport, J. Pharm. Pharm. Sci. 28 (2005) 54–62.
[40] M. Samochocki, A. Höffle, A. Fehrenbacher, R. Jostock, L. Ludwig, C. Christner, M. Radina, M. Zerlin, M. Ullmer, E. Pereira, H. Lübbert, E. Albuquerque, A. Maelicke, Galantamine is an allosterically potentiating ligand of neuronal nicotinic but not of muscarinic acetylcholine receptors, Neuropharmacology 305 (2003) 1024–1036.
[41] I. van den Beukel, R.G. van Kleef, R. Zwart, M. Oortgiesen, Physostigmine and acetylcholine differentially activate nicotinic receptor subpopulations in *Locusta migratoria* neurons, Brain. Res. 789 (1998) 263–273.
[42] B. Katz, S. Thesleff, A study of the desensitization produced by acetylcholine at the motor end-plate, J. Physiol. 138 (1957) 63–80.